



## OPEN ACCESS

## EDITED BY

Gabriela Santos-Gomes,  
New University of Lisbon, Portugal

## REVIEWED BY

Claudia Moreno,  
New University of Lisbon, Portugal  
Arthur de Carvalho e Silva,  
University of Birmingham, United Kingdom

## \*CORRESPONDENCE

Susan A. Charman

✉ [susan.charman@monash.edu](mailto:susan.charman@monash.edu)

John M. Kelly

✉ [john.kelly@lshtm.ac.uk](mailto:john.kelly@lshtm.ac.uk)

Eric Chatelain

✉ [echatelain@dndi.org](mailto:echatelain@dndi.org)

RECEIVED 07 July 2023

ACCEPTED 21 August 2023

PUBLISHED 27 September 2023

## CITATION

Francisco AF, Chen G, Wang W, Sykes ML, Escudié F, Scandale I, Olmo F, Shackleford DM, Zulfiqar B, Kratz JM, Pham T, Saunders J, Hu M, Avery VM, Charman SA, Kelly JM and Chatelain E (2023) Preclinical data do not support the use of amiodarone or dronedarone as antiparasitic drugs for Chagas disease at the approved human dosing regimen.

*Front. Trop. Dis* 4:1254061.

doi: 10.3389/fitt.2023.1254061

## COPYRIGHT

© 2023 Francisco, Chen, Wang, Sykes, Escudié, Scandale, Olmo, Shackleford, Zulfiqar, Kratz, Pham, Saunders, Hu, Avery, Charman, Kelly and Chatelain. This is an open-access article distributed under the terms of the [Creative Commons Attribution License \(CC BY\)](https://creativecommons.org/licenses/by/4.0/). The use, distribution or reproduction in other forums is permitted, provided the original author(s) and the copyright owner(s) are credited and that the original publication in this journal is cited, in accordance with accepted academic practice. No use, distribution or reproduction is permitted which does not comply with these terms.

# Preclinical data do not support the use of amiodarone or dronedarone as antiparasitic drugs for Chagas disease at the approved human dosing regimen

Amanda F. Francisco<sup>1</sup>, Gong Chen<sup>2</sup>, Wen Wang<sup>2</sup>, Melissa L. Sykes<sup>3</sup>, Fanny Escudié<sup>4</sup>, Ivan Scandale<sup>4</sup>, Francisco Olmo<sup>1</sup>, David M. Shackleford<sup>2</sup>, Bilal Zulfiqar<sup>3</sup>, Jadel M. Kratz<sup>4</sup>, Thao Pham<sup>2</sup>, Jessica Saunders<sup>2</sup>, Meiyu Hu<sup>2</sup>, Vicky M. Avery<sup>3</sup>, Susan A. Charman<sup>2\*</sup>, John M. Kelly<sup>1\*</sup> and Eric Chatelain<sup>4\*</sup>

<sup>1</sup>Department of Infection Biology, London School of Hygiene and Tropical Medicine, London, United Kingdom, <sup>2</sup>Centre for Drug Candidate Optimisation, Monash Institute of Pharmaceutical Sciences, Monash University, Parkville, VIC, Australia, <sup>3</sup>Discovery Biology, Centre for Cellular Phenomics, Griffith University, Nathan, QLD, Australia, <sup>4</sup>Drugs for Neglected Diseases initiative (DNDI), Research & Development (R&D), Geneva, Switzerland

The repurposing of approved drugs is an appealing method to fast-track the development of novel therapies for neglected diseases. Amiodarone and dronedarone, two approved antiarrhythmic agents, have been reported to have potential for the management of Chagas disease patients displaying symptomatic heart pathology. More recently, it has been suggested that both molecules not only have an antiarrhythmic effect, but also have trypanocidal activity against *Trypanosoma cruzi*, the causative agent of Chagas disease. In this work, we assessed the *in vitro* activity of these compounds against *T. cruzi*, the *in vivo* pharmacokinetics, and pharmacodynamics, to determine the potential for repurposing these drugs as therapies for Chagas disease. Based on these results, we were unable to reproduce the *in vitro* potencies of amiodarone and dronedarone described in the literature, and both drugs were found to be inactive or cytotoxic against a variety of different mammalian cell lines. The evaluation of *in vivo* efficacy in a bioluminescent murine model of *T. cruzi* did not show antiparasitic activity at the highest tolerated dose tested. While the potential of amiodarone and dronedarone as antiarrhythmic agents in Chagas cardiomyopathic patients cannot be completely excluded, a trypanocidal effect in patients treated with these two drugs appears unlikely.

## KEYWORDS

*Trypanosoma cruzi*, *in vitro*, *in vivo*, bioluminescence imaging, pharmacokinetics, translation, repurposing

## 1 Introduction

The insect-transmitted protozoan parasite *Trypanosoma cruzi* (*T. cruzi*) is the aetiological agent of Chagas disease, and a globally important cause of infectious cardiomyopathy. More than 6 million people in Latin America are currently infected, and due to migration, the disease has also become a public health problem in non-endemic regions, particularly the US and Europe (1–3). Approximately 30% of those infected with *T. cruzi* develop Chronic Chagas Cardiomyopathy (CCC), although symptoms can take many years to become apparent (4). Arrhythmias are the most common initial presentation, often leading to dilated cardiomyopathy, and ultimately to cardiac failure (5, 6). The class III anti-arrhythmic drug amiodarone has been proposed as a therapy for alleviating CCC (7, 8). This benzofuran derivative is widely used to treat and/or mitigate cardiac dysrhythmias, including ventricular tachycardia and atrial fibrillation (9, 10). Amiodarone functions as a broad-spectrum channel blocker ( $K^+$ ,  $Na^+$  or  $Ca^{2+}$ ), and has potent coronary vasodilatory activity. However, there are a wide range of adverse effects, particularly involving the lungs, eye, thyroid, or liver, that can act to restrict its use (11–14).

Dronedarone is produced by Sanofi and sold under the brand name Multaq™ for the treatment of cardiac arrhythmias, in particular to help maintain normal heart rhythms in patients with atrial fibrillation or atrial flutter (heart rhythm disorders) (15). The anti-arrhythmic effects of dronedarone are related to all four classes described in the Vaughan-Williams classification: Class III, dronedarone is a multichannel blocker inhibiting the potassium currents (IK(Ach), IKur, IKr, IKs); Class Ib, dronedarone inhibits the sodium currents; Class IV dronedarone inhibits the calcium currents; and Class II, dronedarone is a non-competitive antagonist of adrenergic activities (16).

The nitroheterocyclic drugs benznidazole and nifurtimox are currently the front-line therapies used against *T. cruzi* infection (17). They can be up to 80% effective in efficacy in achieving sterile cure for both acute and chronic disease (18, 19). Evidence in animal models also suggests that curative treatment can limit the development of CCC, provided that the drugs are administered at an early stage in the infection before the appearance of symptomatic disease (20–22). Both drugs, however, have adverse effects, which combined with long dosing regimens, has impacted negatively on patient compliance. In response to the urgent need for new treatments, there has been an international effort, involving both the academic and commercial sectors, to discover drugs that are more effective and less toxic (23, 24). Several studies have now reported that amiodarone has trypanocidal activity, both *in vitro* and *in vivo*, and that it can act synergistically in combination with the ergosterol biosynthesis inhibitors posaconazole and itraconazole (25–30). The mode of action of amiodarone has been reported to involve disruption of mitochondrial electrochemical potential and alkalization of acidocalcisomes, leading to increased  $Ca^{2+}$  release into the cytosol (28, 31). It also inhibits ergosterol biosynthesis through inhibition of oxidosqualene cyclase (25). There is no experience of the use of dronedarone in Chagas patients.

However, there is evidence that the antiparasitic mechanism of action would be similar to the one described for amiodarone (8, 32).

The dual properties of amiodarone as an anti-arrhythmic drug and a trypanocidal agent has stimulated interest in a ‘kill-two-birds-with-one-stone’ strategy for treating Chagas disease (8). However, in a recent study no differences were found in the parasite load of *T. cruzi* patients who were undergoing anti-arrhythmic treatment with amiodarone compared to non-treated controls (33). This prompted us to re-visit the preclinical evidence for *in vitro* and *in vivo* anti-parasitic efficacy of these benzofuran derivatives. Contrary to previous reports, in our hands, limited selective *in vitro* activity across a variety of different parasite strains and assays methodologies was demonstrated. In addition, we show that neither amiodarone nor dronedarone have an impact on the parasite burden during acute or chronic stage *T. cruzi* infections at an exposure corresponding to the maximum tolerated dose administered. Based on these data, neither compound is predicted to show any anti-parasitic activity in humans with the concentrations achieved using clinical dosing regimens.

## 2 Results

### 2.1 Amiodarone and dronedarone show moderate potency against a panel of *T. cruzi* strains, but lack selectivity against host cells *in vitro*

We first assessed the *in vitro* activity of amiodarone and dronedarone and their respective metabolites desethylamiodarone (DEA) and N-desbutyldronedarone (NDBD) against *T. cruzi* Tulahuen WT (DTU VI) amastigotes in mouse 3T3 fibroblasts (Table 1A). Mean  $IC_{50}$  values of 49  $\mu$ M and 9  $\mu$ M were found for amiodarone and dronedarone respectively. Interestingly, both metabolites are nearly equipotent compared to the parent compounds when run in parallel in the same assay (mean  $IC_{50}$  of 28  $\mu$ M for DEA and 10  $\mu$ M for NDBD) although both metabolites showed poor selectivity to host cells. However, both drugs, and in particular amiodarone, had moderate to no selectivity index (SI) over the 3T3 cells used in the assay (SI values varying between 0.75 and 1.5 for amiodarone and 3.2 and 7.8 for dronedarone (Table 1A), thus diminishing the therapeutic potential of these drugs.

To get a broader idea of the potential of these two drugs, *in vitro* data were also generated in amastigote intracellular inhibition assays using *T. cruzi* strains representative of various Discrete Typing Units (DTU): JR and Sylvio X10 strains both belonging to DTU I, Y strain (DTU II) and CL Brener strain (DTU VI). In all cases benznidazole was assessed in parallel as a positive control ( $IC_{50}$  ranging from 2–10  $\mu$ M). Overall, the averaged  $IC_{50}$  values ( $\mu$ M; mean  $\pm$  SD) for amiodarone and dronedarone were 11.2  $\pm$  15.6 and 4.1  $\pm$  2.8 respectively, while the  $IC_{90s}$  ( $\mu$ M; mean  $\pm$  SD) were 17.2  $\pm$  15.2 and 6.4  $\pm$  4.4, respectively (Tables 1A, B). Importantly, in each assay, all available calculated SI values highlighted the relatively low selectivity over the mammalian cell lines used (SI ranging from 0.75 to 7.2 for amiodarone and 0.6 to 7.8

**TABLE 1** *In vitro* potency of amiodarone, dronedarone and their respective metabolites DEA and NDBD against *T. cruzi* infected host cells following 48 hours incubation.

(A) The IC<sub>50</sub> values of amiodarone, dronedarone and their main metabolites against *T. cruzi* Tulahuen WT (DTU VI) amastigotes in mouse 3T3 fibroblasts, and against the 3T3 host cells themselves.

Compound	IC <sub>50</sub> (μM +/- SD)	SI
Amiodarone	48.8 +/- 6.8	0.75-1.5*#
Desethylamiodarone (DEA)	28.1 +/- 5.5	1.3-2.6*
Dronedarone	9.3 +/- 0.4	3.2-7.8*
N-desbutyldronedarone (NDBD)	10.6 +/- 3.1	0.88
Benznidazole	9.7 +/- 1.5	>13

\* No curve fit possible for cytotoxicity data (no upper plateau) – 2 concentrations around estimated CC50 used for SI calculation. Values were determined from two experimental replicates, with duplicate technical replicates per experiment. # No curve fit possible for *T. cruzi* activity (no upper plateau), with a mean activity of 93% at the highest assay concentration of 73 μM. The IC<sub>50</sub> value was predicted, using Prism 6. See Griffith assay in [Supplementary Material](#) for more details.

B) Potency against intracellular amastigotes of different *T. cruzi* intracellular strains and selectivity towards their corresponding and varied host cells.

Parasite strain (DTU)/host cell	Amiodarone			Dronedarone		
	IC <sub>50</sub> μM (mean +/-SD)	IC <sub>90</sub> μM (mean +/-SD)	Selectivity Index	IC <sub>50</sub> μM (mean +/-SD)	IC <sub>90</sub> μM (mean +/-SD)	Selectivity Index
Tulahuen Cl2 (VI)/MRC5	3.6 +/- 2.6	6.1 +/- 4.5	2.2	1.2 +/- 0.7	3.9 +/- 0.0	2.4
Y strain (II)/U2OS	6.2 +/- 1.5	22.8 +/- 7.2	1.3	NT	NT	NT
Silvio X10/7A1 (I)/Vero	2.0 +/- 0.3	3.6 +/- 2.1	4.4	NT	NT	NT
Tulahuen Cl2 (VI)/L6	10.8 +/- 2.9	19.5 +/- 4.7	1.2	4.8 +/- 0.1	ND	0.6
CL Brener(VI)/COLO-N680	2.5*	8.0*	7.2	1.7*	3.8*	6.8
JR (I)/COLO-N680	4.5*	9.5*	4.1	3.3*	3.8*	3.5

The IC<sub>50</sub> values against various *T. cruzi* strains (Discrete Typing Units or DTUs) and host cells were determined as outlined (Methods). Benznidazole (BZ) was included as a reference drug. Values were obtained from >2 (or 2\*) independent experiments, with 3 technical replicates per concentration. Selectivity indices (SI) were calculated from the ratio host cell:parasite IC<sub>50</sub> values. SD, Standard deviation; ND, Not determined; NT, Not tested; \*: 3 technical replicates.

for dronedarone). Selectivity should always be considered in the interpretation of *in vitro* activity of compounds to identify the negative effect of compounds on mammalian host cells. The consistency of this finding of minimal selectivity, irrespective of the parasite strain, specific host cell used or methodology, highlights the fundamental issues with these drugs in treating Chagas disease.

The *in vitro* activity of amiodarone and dronedarone was also determined against epimastigotes, the insect form of the *T. cruzi* parasite, and were found to be within the same μM range demonstrated for amastigotes (see [Supplementary Table S1](#)). Interestingly, both drugs were more potent than benznidazole against the epimastigote stage of the parasite.

## 2.2 Amiodarone and dronedarone are inactive in an *in vivo* model of *T. cruzi* infection

To assess *in vivo* efficacy, we first determined the impact of amiodarone and dronedarone on acute stage murine infections with *T. cruzi* CL Brener (DTU VI) and JR (DTU I) in BALB/c mice using bioluminescence imaging. BALB/c mice at the peak of the acute stage (day 14 post-infection) were treated with 5 daily oral doses of

75 mg kg<sup>-1</sup> amiodarone or with 100 mg kg<sup>-1</sup> dronedarone (same batches as those used in the *in vitro* studies to eliminate potential effects of batch variation). Neither of the treatment schedules used had any significant effect on the bioluminescence-inferred parasite burden in acute stage disease irrespective of the *T. cruzi* strain used ([Figure 1](#)).

In contrast, parallel treatment of infected mice with the front-line drug benznidazole (100 mg kg<sup>-1</sup>) reduced the parasite burden by >99.9%, close to the limit of detection. To further explore the potential anti-*T. cruzi* activity of amiodarone and dronedarone, we then treated mice during the chronic stage of infection with the CL Brener strain (104 days post-infection) when immune pressure had reduced the parasite burden by more than 2 orders of magnitude ([Figure 2](#)).

We did not observe any significant reduction in parasitemia at the end of a 5-day treatment regimen in the chronic BALB/c infection model with the *T. cruzi* CL strain. Therefore, highly sensitive bioluminescence imaging demonstrates that neither amiodarone or dronedarone has significant activity against acute or chronic stage *T. cruzi* infections at the doses used. In contrast, treatment with benznidazole as a positive control reduced the parasite burden close to the limit of detection as expected. This benznidazole treatment schedule is curative when applied to

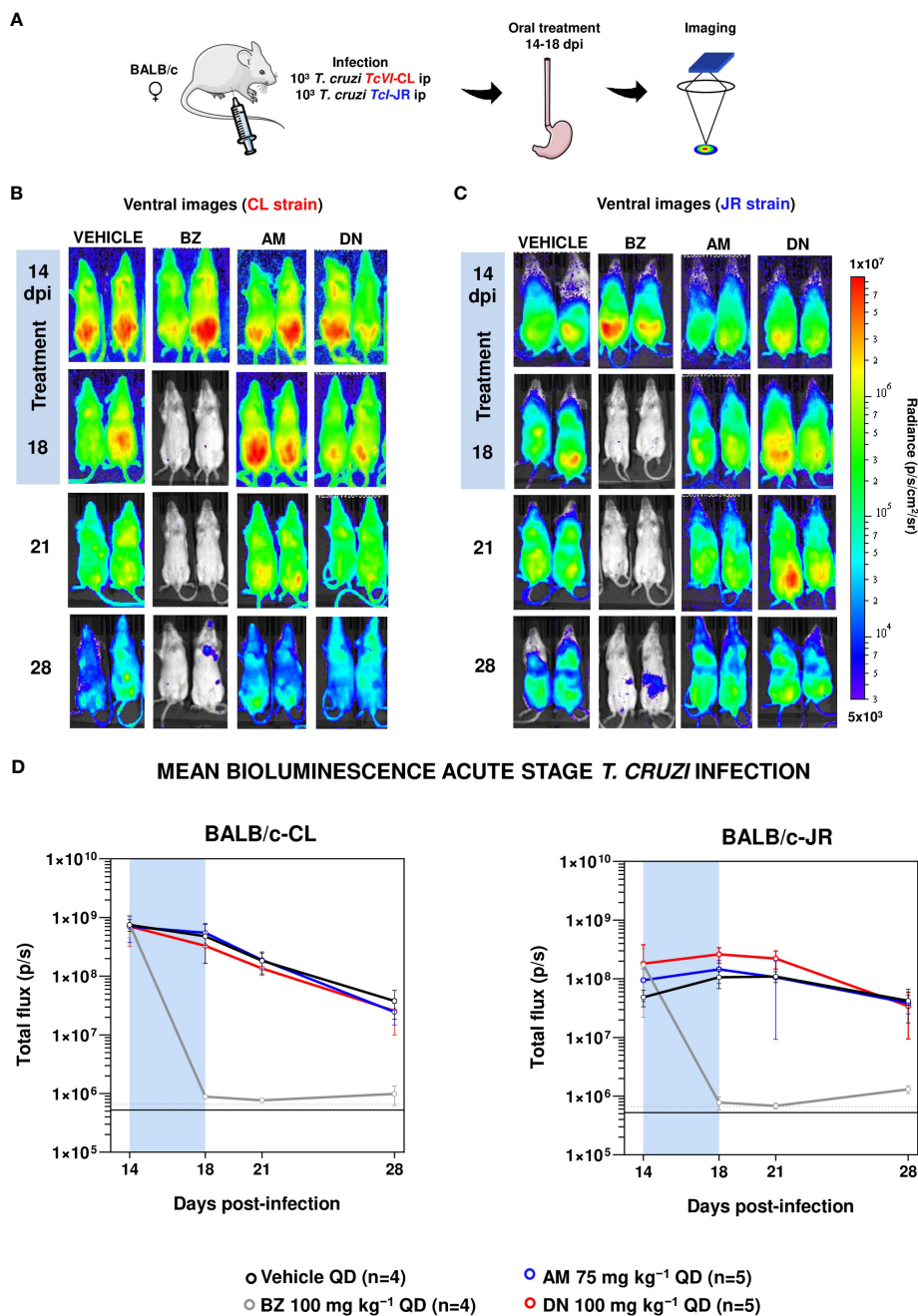


FIGURE 1

Amiodarone and dronedarone are ineffective against acute stage *T. cruzi* infections. (A) Study strategy. Parts of the figure were drawn using pictures from Servier Medical Art. Servier Medical Art by Servier is licensed under a Creative Commons Attribution 3.0 Unported License (<https://creativecommons.org/licenses/by/3.0/>). (B, C) BALB/c mice, infected with bioluminescent *T. cruzi* CL Brener (B) and JR parasites (C), were treated 14 days post-infection (dpi), once daily by oral gavage for 5 days; with 100 mg kg<sup>-1</sup> benznidazole (BZ) (n=4), 75 mg kg<sup>-1</sup> amiodarone (AM) (n=5), or with 100 mg kg<sup>-1</sup> dronedarone (DN) (n=5). Representative ventral images of two mice per group are shown, at the dpi indicated. The heat-map is on a log<sub>10</sub> scale and indicates intensity of bioluminescence from low (blue) to high (red); the minimum and maximum radiances for the pseudocolour scale are shown. (D) Graphs showing the mean bioluminescence (p/s) determined by *in vivo* imaging of mice infected with CL Brener (left graph) or JR strain (right graph) parasites (Methods). Treatment groups, dosing regimens, including time of treatment (blue bar), are indicated. The horizontal unbroken line indicates background bioluminescence established from non-infected mice, with the dashed line indicating 2 × SD above the mean.

chronic stage infections (34). Given the modest *in vitro* activity, the limited selectivity over mammalian cells (Table 1), the poor drug exposure (see Figure 3, Table 2 below), and the lack of *in vivo* activity against the CL Brener and JR strains (Figures 1, 2), further animal experimentation was not undertaken.

### 2.3 Amiodarone and dronedarone exposure in mice

In parallel to the *in vivo* efficacy studies, the exposure of amiodarone and dronedarone was assessed in non-infected female

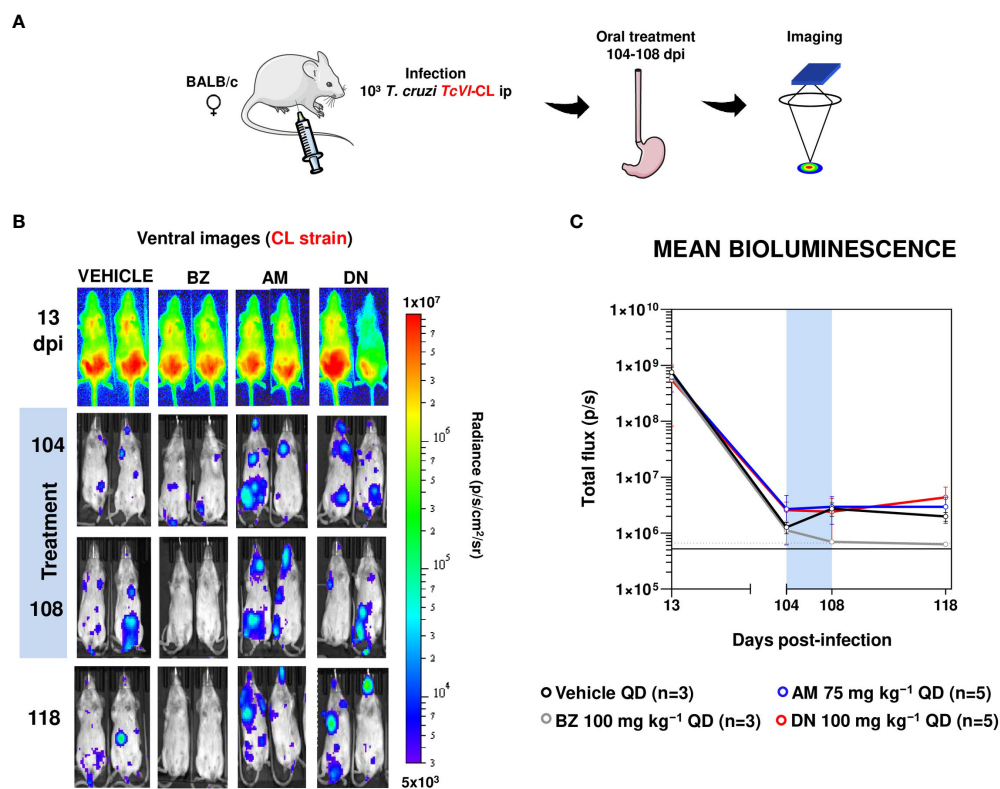


FIGURE 2

Amiodarone and dronedarone are ineffective against chronic stage *T. cruzi* infections. (A) Study strategy. Parts of the figure were drawn using pictures from Servier Medical Art. Servier Medical Art by Servier is licensed under a Creative Commons Attribution 3.0 Unported License (<https://creativecommons.org/licenses/by/3.0/>). (B) Representative ventral images of BALB/c mice infected with bioluminescent *T. cruzi* CL Brener and treated once daily for 5 days with 100 mg kg<sup>-1</sup> benznidazole (BZ) (n=3), 75 mg kg<sup>-1</sup> amiodarone (AM) (n=5), or with 100 mg kg<sup>-1</sup> dronedarone (DN) (n=5), starting 104 days post-infection (dpi). Mice were imaged, as in Figure 1. (C) Graph showing the mean bioluminescence of the infected and treated mice. Treatment groups, dosing regimens, including treatment period (blue bar) are indicated.

BALB/c mice following oral administration at the same doses (75 and 100 mg kg<sup>-1</sup>, respectively) and using the same formulation as for the *in vivo* efficacy studies. Plasma protein binding in mouse and human plasma and binding to the *in vitro* testing medium were also measured to determine the respective unbound concentrations.

Plasma concentration versus time profiles is shown in Figure 3 and pharmacokinetic and binding properties are tabulated in Table 2.

Amiodarone was detected in plasma for the duration of the 48 h sampling period. The apparent half-life was long (15 h), however

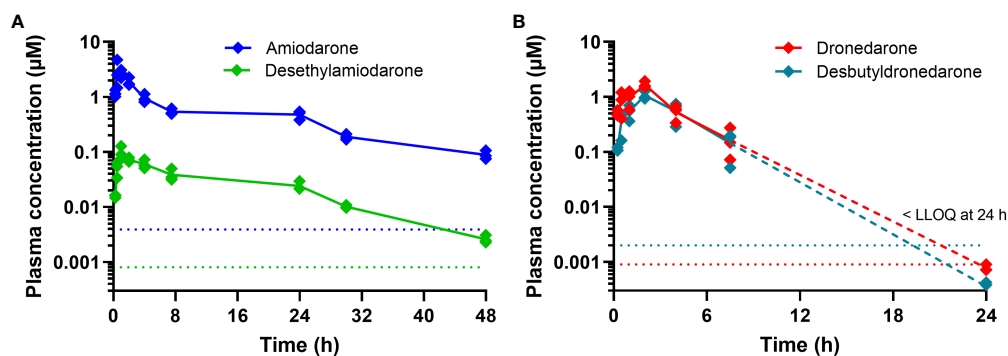


FIGURE 3

Plasma concentration versus time profiles for (A) amiodarone and DEA and (B) dronedarone and N-desbutyldronedarone following oral dosing to non-infected female BALB/c mice at doses of 75 and 100 mg kg<sup>-1</sup>, respectively, of the parent compounds. Each data point represents the average of n=3 concentrations at each time point ( $\pm$  SD) and dotted lines represent the respective analytical lower limit of quantitation (LLOQ). Note that for dronedarone and N-desbutyldronedarone, the concentrations at 24 h were either at or below the LLOQ and should be considered as estimates only [dashed lines in (B)].

TABLE 2 Pharmacokinetic properties of amiodarone and dronedarone and the primary metabolites, DEA and N-desbutyldronedarone, in non-infected female BALB/c mice following oral administration.

Parameter	Amiodarone	Dronedarone
Dose (mg kg <sup>-1</sup> )	75	100
Half-life (h)	15	2.1
Plasma AUC <sub>inf</sub> (μM.h)	24	5.6
C <sub>max</sub> (μM)	2.9	1.7
Unbound C <sub>max</sub> (nM)	0.87	5.3
T <sub>max</sub> (h)	0.5	2.0
C <sub>24 h</sub> (μM)	0.480	0.001
Unbound C <sub>24 h</sub> (nM)	0.14	0.0031
Metabolite Half-life (h)	10	1.9
Metabolite Plasma AUC <sub>inf</sub> (μM.h)	1.2	4.1
Metabolite C <sub>max</sub> (μM)	0.098	1.1
Metabolite T <sub>max</sub> (h)	1.0	2.0
Fraction parent unbound in mouse plasma	0.00030 ± 0.00002	0.0031 ± 0.0004
Fraction parent unbound in human plasma	0.00024 ± 0.00001	0.0016 ± 0.0004
Fraction parent unbound in <i>in vitro</i> medium	0.013 ± 0.0009	0.194 ± 0.021

Note that unbound concentrations (C<sub>max</sub> and C<sub>24 h</sub>) are expressed in nM whereas all other concentrations are expressed in μM. All values are based on the mean of n=3 measurements per time point. The fraction unbound in mouse and human plasma, and in the *in vitro* testing medium is also shown (mean ± SD).

this is an approximate value only as the terminal phase was not clearly defined by the available data. Maximum plasma concentrations were observed at 0.5 h indicative of rapid absorption. At 24 h (at which time the next dose was administered in the efficacy study), the concentration of amiodarone was ~0.48 μM. The primary metabolite, DEA, was also detected in plasma for the duration of the sampling period, however plasma exposure was low (C<sub>max</sub> < 0.1 μM, Figure 3, Table 2).

Dronedarone plasma concentrations were detected up to 24 h post dose, but concentrations were at the LLOQ (~0.001 μM) at the 24 h time point. The half-life was approximately 2 h and maximum plasma concentrations were observed at 2 h post dose. Plasma

concentrations of the primary metabolite, NDBD, were comparable to concentrations of the parent compound and were below the LLOQ at the 24 h time point (Figure 3, Table 2).

Plasma protein binding studies indicated very high binding in both species, with >99.97% bound for amiodarone and >99.7% bound for dronedarone. These results are consistent with data previously reported for amiodarone binding in human plasma (35). To assess the likely concentration present over the full 5-day dosing period, amiodarone and dronedarone single dose concentration versus time profiles (Figure 3) were fitted to a 2-compartment model with first order absorption and elimination (Figure S1). Repeat dose profiles were then simulated with the assumption that there were no changes to the PK properties

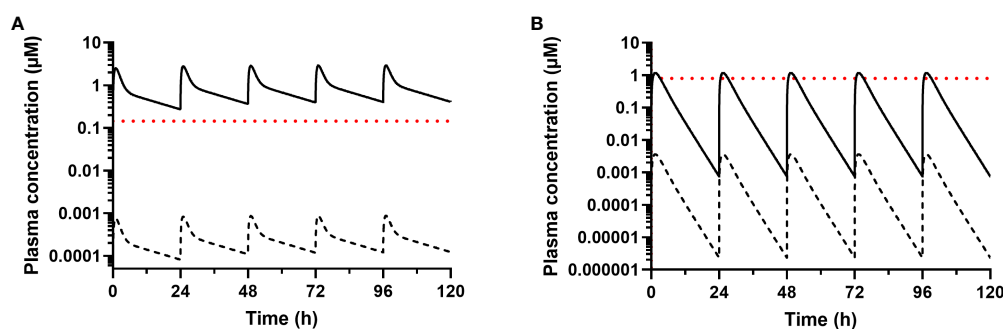


FIGURE 4

Simulated total (solid line) and unbound (dashed line) plasma concentrations after once daily dosing of (A) amiodarone and (B) dronedarone at 75 and 100 mg kg<sup>-1</sup>, respectively, to non-infected female BALB/c mice. The calculated unbound *in vitro* IC<sub>50</sub> values were calculated from the aggregate IC<sub>50</sub> (Table 1) and the fraction unbound in media (Table 2) and are shown for comparison (red dotted lines, 0.15 μM for amiodarone or 0.80 μM for dronedarone). The unbound plasma concentrations were calculated using the fraction unbound values shown in Table 2.

following repeat administration. Figure 4 shows the simulated profiles for the total (solid lines) and unbound (dashed lines) plasma concentrations for both compounds along with the unbound *in vitro* IC<sub>50</sub> value for reference (red dotted lines).

### 3 Discussion

A potential intrinsic antiparasitic effect of amiodarone and dronedarone has been suggested during the last two decades using different *in vitro* and *in vivo* studies (8, 32). Such a scenario could be highly beneficial as these anti-arrhythmic drugs are also used to treat patients with CCC. These reported results, however, are overshadowed by clinical data generated almost a decade ago showing no benefit in Chagas patients undergoing anti-arrhythmic treatment with amiodarone; indeed, no differences were found in the parasite load of amiodarone-treated patients compared to non-treated patients (33). This prompted us to revisit the preclinical evidence supporting any potential antiparasitic role for amiodarone and dronedarone in Chagas patients.

To determine if amiodarone and dronedarone were selective antiparasitic agents against the intracellular form of *T. cruzi*, *in vitro* data were generated in a range of different assays (e.g. different *T. cruzi* strains and host cells, different multiplicity of infection, different incubation times, different times of addition of trypomastigotes to infect cells) and compared to previous literature (25–31). In addition, these compounds were tested against Tulahuen strain epimastigotes. Data from our *in vitro* studies showed a good degree of correlation between the IC<sub>50</sub> values generated here with previously reported data. Of note, these compared favorably with *in vitro* data generated using *T. cruzi* epimastigotes, the insect stage of the parasite, in line with previous reports (28).

Further interrogation of the available collective data indicated relatively poor activity for both compounds, but more specifically for amiodarone (50 μM in the standard *T. cruzi* Tulahuen WT (DTU VI) amastigotes assay in mouse 3T3 fibroblasts). This would not be considered even as a “hit” with currently accepted *in vitro* criteria for *T. cruzi*: IC<sub>50</sub> < 5 μM ideally 1 μM and; SI > 10 ideally 100 (36). Of greater concern was the lack of selectivity towards the host cells demonstrated by all evaluations undertaken, shedding further doubt on the potential suitability of these drugs for the treatment of *T. cruzi* infections. When we tested both compounds *in vivo* in the well-established and standardized bioluminescent imaging (BLI) model (37), no efficacy was observed either in the acute or chronic model of *T. cruzi*. These data are in sharp contrast to former studies claiming a potential benefit of the treatment with these compounds, alone, or in combination with azoles in murine or canine models of *T. cruzi* infection (25, 38, 39).

Given these results, we also assessed the exposure in mice for both amiodarone and dronedarone and their main metabolites at the doses used in *in vivo* efficacy studies to see if adequate concentrations relative to the *in vitro* IC<sub>50</sub> values were achieved. Plasma exposure of amiodarone was high, and the half-life was long following oral administration of 75 mg kg<sup>-1</sup> to mice. Given the very high plasma protein binding of amiodarone, unbound

concentrations were very low (C<sub>max</sub> < 1 nM) and considerably below the *in vitro* unbound IC<sub>50</sub> values (~0.15 μM, Figure 3). While the active metabolite DEA was also detected, concentrations were approximately 20-fold lower than for the parent compound. At a dose of 100 mg kg<sup>-1</sup>, dronedarone had lower overall exposure and a much shorter half-life than amiodarone (Figures 3, 4). Even though the plasma protein binding of dronedarone is lower than that for amiodarone, unbound concentrations (C<sub>max</sub> < 5 nM) were still likely to be below the unbound IC<sub>50</sub> (~0.8 μM) for the duration of the dosing period (Figure 3).

N-desbutyldronedarone was detected in mouse plasma and concentrations were comparable to those for dronedarone. However, as for dronedarone, unbound concentrations would have likely been too low to see an antiparasitic effect. Collectively, the exposure results suggest that concentrations of amiodarone and dronedarone (as well as their main metabolites) at tolerated doses were insufficient to elicit any notable effect on parasites in this murine model. As exposure in the mouse would not reach close to the IC<sub>50</sub>, not to mention the IC<sub>90</sub> of these drugs, it raises questions regarding the data generated by others in murine models, and thus the potential influence of the different models in our interpretation of the data. It also highlights the importance of generating PK data in the animal species used for PD studies with compounds of interest. Even though the duration of treatment in some of the published studies was much longer than that used in our studies (15 days dosing every other day in ref 25, for example), concentrations would not have reached levels required for efficacy. Indeed, the current expectation in drug discovery for Chagas disease is that a minimum sustained unbound exposure above the IC<sub>90</sub> is needed throughout the treatment duration to observe any curative effect in the animals (depending on the mechanism of action). Moreover, the doses tested in our work were similar to or higher than those tested previously.

The extrapolation of these results for amiodarone in mice to the clinical situation is complicated due to the highly variable nature of amiodarone's absorption and pharmacokinetics. It has a very long half-life and can have adverse effects in humans, all of which require complex dosing regimens and individual patient titration. For example, to achieve an anti-arrhythmic effect with amiodarone, administration of a loading dose ranging from 800 to 1,600 mg day<sup>-1</sup> is often used over the first 1-3 weeks, followed by a maintenance dose of 600 to 800 mg day<sup>-1</sup> for a month, before a further dose reduction to 400 mg day<sup>-1</sup> (40). Given that the target clinical steady state concentration range for amiodarone to achieve the desired anti-arrhythmic effect and minimize serious side effects (40, 41) is 1-2.5 mg L<sup>-1</sup> (or 1.6-3.9 μM), average unbound concentrations would be less than 1 nM which is at least 150- or 220-fold below the estimated unbound IC<sub>50</sub> (0.15 μM) or IC<sub>90</sub> (0.22 μM), respectively. Even if one takes into consideration the similar potency of amiodarone and its primary metabolite against *T. cruzi*, the total exposure for this drug would still be well below that needed to reach the IC<sub>50</sub> not to mention the IC<sub>90</sub>. Notwithstanding these arguments, there is evidence showing that amiodarone can accumulate in certain human tissues (42, 43), and therefore one cannot unequivocally exclude that in some local tissues or regions, amiodarone concentrations could potentially reach effective levels.

However, it seems unlikely, given the dynamic character of the *T. cruzi* infection, that this would lead to parasite eradication.

For dronedarone, the only recommended dose in humans for the paroxysmal or persistent atrial fibrillation or atrial flutter is 800 mg daily Multaq<sup>TM</sup> in adults (44). At this dose, steady-state plasma concentrations ranging from 0.2–0.3  $\mu\text{M}$  (unbound concentrations < 1 nM) are reached in 7 days (45). Again, this exposure for dronedarone (and its major metabolite) in humans using a standard dosing regimen is far below that needed to reach the estimated unbound *in vitro* IC<sub>50</sub> (0.8  $\mu\text{M}$ ) or IC<sub>90</sub> (1.2  $\mu\text{M}$ ) observed against *T. cruzi*.

In summary, based on *in vitro* and *in vivo* activity data, along with exposure and consideration of unbound concentrations, our data do not support the likelihood of an antiparasitic effect of amiodarone or dronedarone in humans and are in line with preliminary clinical data showing no effect of these drugs on *T. cruzi* parasite load in Chagas disease patients (33). This study also emphasizes the importance and impact of the scientific methodology and data analysis used, and the interpretation of the outcomes generated in the context of the feasibility and potential of repurposing strategies of existing drugs for new indications.

## 4 Methods

### 4.1 Compounds

Amiodarone HCL, its metabolite DEA and dronedarone HCL, used for *in vitro* and *in vivo* studies, were purchased from AK Scientific, Union City, USA. Dronedarone metabolite, aka N-desbutyldronedarone, was purchased from BDG Synthesis, Wellington, New Zealand. Compounds were dissolved in dimethylsulfoxide (DMSO) to 10 mM stock solutions. Amiodarone HCL and dronedarone HCL were formulated as a 2.5 to 10 mg ml<sup>-1</sup> suspension (depending on dose) in a vehicle containing 0.5% (w/v) hydroxypropyl methylcellulose (HPMC) and 0.4% (v/v) Tween 80 in Milli-Q H<sub>2</sub>O. Benznidazole, was synthesized by Epichem Pty Ltd., Bentley, Australia.

### 4.2 *In vitro* assessment of compound activity

Direct comparison of the *in vitro* potency of amiodarone, dronedarone and their respective metabolites DEA and NDBD (Table 1A) against *T. cruzi* Tulahuen WT (DTU VI) amastigotes in mouse 3T3 fibroblasts, was performed as described earlier (46).

*In vitro* potency of amiodarone and dronedarone against different *T. cruzi* intracellular amastigotes and selectivity towards various host cells (Table 1B) was determined using several different assays (different host cells, multiplicity of infection, parasite strain, drug incubation time and endpoint used e.g. HCS), and performed in different laboratories. Detailed information of the methods used has been published previously (47–50). When presented as averaged IC<sub>50</sub> and IC<sub>90</sub> values, data from amastigote intracellular inhibition assays was calculated as the mean value obtained from 3–5 different

assays. Determination of the *in vitro* potency of amiodarone and dronedarone against epimastigotes and amastigotes forms of the parasites used in the *in vivo* studies was performed as described previously (50, 51).

### 4.3 Mice and parasites

Animal infections were performed under UK Home Office licence PPL P9AEE04E4 and approved by the London School of Hygiene and Tropical Medicine Animal Welfare and Ethical Review Board (AWERB). All protocols and procedures were conducted in accordance with the UK Animals (Scientific Procedures) Act 1986. Female BALB/c mice were obtained from Charles River (UK) and CB17 SCID mice were bred in-house. BALB/c mice aged 7–8 weeks were maintained in groups of 3, 4 or 5, where they experienced a 12-hour light/dark cycle and had access to food and water *ad libitum*. At time points indicated, mice were infected with bioluminescent *T. cruzi* CL Brener or JR strains engineered to express a red-shifted luciferase that facilitates highly sensitive non-invasive monitoring of the parasite burden in real-time (52, 53). Typically, 1 × 10<sup>4</sup> bloodstream trypomastigotes (BTs) in 0.2 ml PBS were used to infect SCID mice via intraperitoneal (i.p.) inoculation. Parasitaemic blood from these mice was obtained 17 (CL Brener) and 20 (JR) days later and adjusted to 5 × 10<sup>3</sup> BTs ml<sup>-1</sup> with Dulbecco's Ca<sup>2+</sup>/Mg<sup>2+</sup> free PBS (D-PBS). BALB/c mice were then infected i.p. with 1 × 10<sup>3</sup> BTs. Amiodarone and dronedarone were prepared for administration in an aqueous suspension vehicle containing 0.5% (w/v) hydroxypropyl methylcellulose and 0.4% (v/v) Tween 80. The dosing regimens were selected based on previously published *in vivo* work (25, 38). Drugs were administered by oral gavage (adjusted by weight), and vehicle only was administered to control mice.

### 4.4 *In vivo* bioluminescence imaging

Mice were injected i.p. with 150 mg kg<sup>-1</sup> d-luciferin in D-PBS, then anaesthetized using 2.5% (v/v) isoflurane in oxygen for 2–3 minutes. Images were obtained using an IVIS Spectrum system (Caliper Life Sciences) 5–10 minutes after d-luciferin administration. Exposure times varied from 10 seconds to 5 minutes, depending on signal intensity. To estimate parasite burden, whole body regions of interest were drawn using Living Image<sup>®</sup> 4.5.5 to quantify bioluminescence expressed as total flux (photons/second; p/s). The detection threshold was established from uninfected mice.

### 4.5 Pharmacokinetic assessment in mice

Pharmacokinetic studies in non-infected mice were conducted at Monash University using established procedures in accordance with the Australian Code of Practice for the Care and Use of Animals for Scientific Purposes, and the study protocols were reviewed and approved by the Monash Institute of Pharmaceutical Sciences Animal Ethics Committee. Female BALB/c mice (17–21 g) were



obtained from the Monash Animal Research Platform and mice had access to food and water *ad libitum* throughout the pre- and post-dosing periods.

Amiodarone and dronedarone were formulated for oral administration as suspensions in 0.5% (w/v) hydroxypropyl methylcellulose, 0.5% benzyl alcohol, and 0.4% (v/v) polysorbate 80 in water. Compounds were dosed orally by gavage (0.2 mL per mouse). Blood samples were collected up to 24–48 h ( $n = 3$  mice per time point) with a maximum of three samples from each mouse. Samples were collected via submandibular bleed (approximately 120  $\mu$ L). Blood was collected into polypropylene Eppendorf tubes containing heparin as anticoagulant and centrifuged immediately for the separation of plasma, which was stored at  $-80^{\circ}\text{C}$  until analysis by LC-MS.

Plasma sample and standard analysis was conducted using LC/MS/MS following protein precipitation with acetonitrile (4- or 5-fold volume ratio). Blank mouse plasma was used to prepare calibration standards over the concentration range of 2.5–10,000  $\text{ng mL}^{-1}$  (amiodarone) or 0.5–5000  $\text{ng mL}^{-1}$  (dronedarone) and diazepam was added as an internal standard. Following protein precipitation, samples were centrifuged and the supernatant collected for analysis. Samples and standards (1  $\mu$ L) were injected onto a Supelco AscentisExpress RP C8 (amiodarone, desethylamiodarone) or RP amide (dronedarone, N-desbutyldronedarone) column (50 x 2.1 mm, 2.7  $\mu$ m) and eluted using a mobile phase of 0.05% formic acid in water and 0.5% formic acid in acetonitrile mixed using a gradient from 5 to 95% (amiodarone, desethylamiodarone), or 10 to 80% (dronedarone, N-desbutyldronedarone) acetonitrile, over a 4 min cycle time with a flow rate of 0.4  $\text{mL min}^{-1}$ . The LCMS system included a Waters Xevo TQD MS coupled to a Waters Acquity UPLC. Sample detection was conducted using positive electrospray ionization in multiple reaction monitoring mode. The MS/MS transitions were 646.03 > 100.07 (cone voltage of 60 V, CID 30V) for amiodarone, 618.07 > 72.05 (cone voltage of 55 V, CID 25V) for desethylamiodarone, 557.36 > 100.04 (cone voltage of 75 V, CID 40 V) for dronedarone, 501.27 > 114.09 (cone voltage of 60 V, CID 35 V) for N-desbutyldronedarone and 285.12 > 154.09 (cone voltage of 50 V, CID of 25 V) for diazepam. Assays were validated for linearity, matrix effects, accuracy, precision and recovery.

Plasma concentration versus time data were analyzed using standard non-compartmental methods and were also fitted with a two compartment (amiodarone) or one compartment (dronedarone) model with first order absorption and elimination using PK Solver (ver 2.0). A weighting factor of  $1/\text{concentration}^2$  provided the best fit to the experimental data. Using the derived PK parameters, repeat dose profiles were simulated assuming no change to the PK properties upon repeat dosing (i.e. minimal enzyme inhibition or induction).

## 4.6 Plasma and media binding

Protein binding was determined in diluted plasma via rapid equilibrium dialysis with incorporation of a pre-saturation step

based on methods reported previously (35). Prior to the dialysis experiment, RED inserts (Thermo Fisher Scientific Inc.) were presaturated by adding solutions containing each compound (at 500 nM in isotonic phosphate buffered saline (PBS), pH 7.4) to both the donor and the dialysate chambers and incubating at  $37^{\circ}\text{C}$  on an orbital plate shaker (450 rpm; ThermoMixer C, Eppendorf) for 2 x 30 min cycles and an overnight cycle. At the end of each presaturation cycle, solutions from both donor and dialysate chambers were removed and discarded. Following the presaturation, diluted human and mouse plasma (10% v/v in pH 7.4 PBS) were spiked with each compound (at 5000 nM) and dialyzed against pH 7.4 PBS containing a low concentration of compound (100 nM) for 24 h. Concentrations of each compound in dialysate and donor samples collected at the end of the dialysis period were determined via LC-MS as described above. Compound binding was assessed on the basis of the measured concentrations in dialysate and donor samples at the end of the dialysis period assuming that the system was at steady state by 24 h. As the binding assay was performed using diluted plasma, data were corrected for the dilution factor to give a binding value for neat matrix via an established approach which accounts for the shift in equilibria that occurs with protein dilution (54).

## Data availability statement

The raw data supporting the conclusions of this article will be made available by the authors, without undue reservation.

## Ethics statement

Animal infections were performed under UK Home Office licence PPL P9AEE04E4 and approved by the London School of Hygiene and Tropical Medicine Animal Welfare and Ethical Review Board (AWERB). All protocols and procedures were conducted in accordance with the UK Animals (Scientific Procedures) Act 1986. Pharmacokinetic studies in non-infected mice were conducted at Monash University using established procedures in accordance with the Australian Code of Practice for the Care and Use of Animals for Scientific Purposes, and the study protocols were reviewed and approved by the Monash Institute of Pharmaceutical Sciences Animal Ethics Committee. The study was conducted in accordance with the local legislation and institutional requirements.

## Author contributions

AF: Formal Analysis, Investigation, Methodology, Writing – review & editing. GC: Investigation, Writing – review & editing. WW: Investigation, Writing – review & editing. MS: Formal Analysis, Investigation, Methodology, Writing – review & editing. FE: Formal Analysis, Writing – review & editing. IS: Formal Analysis, Writing – review & editing. FO: Formal Analysis, Investigation, Writing – review & editing. DS: Formal Analysis,

Supervision, Writing – review & editing. BZ: Formal Analysis, Investigation, Writing – review & editing. JaK: Writing – review & editing. TP: Investigation, Writing – review & editing. JS: Investigation, Writing – review & editing. MH: Investigation, Writing – review & editing. VA: Formal Analysis, Methodology, Supervision, Writing – review & editing. SC: Formal Analysis, Methodology, Supervision, Writing – original draft, Writing – review & editing. JoK: Supervision, Writing – original draft, Writing – review & editing. EC: Project administration, Supervision, Writing – original draft, Writing – review & editing.

## Funding

This project was carried out and funded through DNDi. For part of this work, DNDi received funding from the Federal Ministry of Education and Research (BMBF) through KfW (Germany), the Foreign Commonwealth & Development Office (FCDO, UK), Directorate-General for International Cooperation (DGIS), The Netherlands; Swiss Agency for Development and Cooperation, Switzerland; and for its overall mission from Médecins Sans Frontières (Doctors Without Borders), International. The donors had no role in the study design, data collection and analysis, decision to publish, or preparation of the manuscript. *In vitro* and *in vivo* pharmacokinetic studies at the Centre for Drug Candidate Optimisation, Monash University were supported in part by the DNDi, Monash University Technology Research Platform network and Therapeutic Innovation Australia (TIA) through the Australian Government National Collaborative Research Infrastructure Strategy (NCRIS) program. *In vitro* parasitology undertaken by Discovery Biology, Griffith University were supported by DNDi and Griffith University.

## References

- World Health Organisation. *Chagas disease (also known as American trypanosomiasis)* (2021). Available at: [https://www.who.int/news-room/fact-sheets/detail/chagas-disease-\(american-trypanosomiasis\)](https://www.who.int/news-room/fact-sheets/detail/chagas-disease-(american-trypanosomiasis)) (Accessed June 20, 2023).
- Manne-Goehler J, Umeh CA, Montgomery SP, Wirtz VJ. Estimating the burden of Chagas disease in the United States. *PLoS Negl Trop Dis* (2016) 10:e0005033. doi: 10.1371/journal.pntd.0005033
- Antinori S, Galimberti L, Bianco R, Grande R, Galli M, Corbellino M. Chagas disease in Europe: A review for the internist in the globalized world. *Eur J Intern Med* (2017) 43:6–15. doi: 10.1016/j.ejim.2017.05.001
- Viotti R, Vigliano CA, Álvarez MG, Lococo BE, Petti MA, Bertocchi GL, et al. The impact of socioeconomic conditions on chronic Chagas disease progression. *Rev Esp Cardiol* (2009) 62(11):1224–32. doi: 10.1016/S0300-8932(09)73074-X
- Tanowitz HB, MaChado FS, Spray DC, Friedman JM, Weiss OS, Lora JN, et al. Developments in the management of Chagas cardiomyopathy. *Expert Rev Cardiovasc Ther* (2015) 12:1393–409. doi: 10.1586/14779072.2015.1103648
- Bonney KM, Luthringer DJ, Kim SA, Garg NJ, Engman DM. Pathology and pathogenesis of Chagas heart disease. *Annu Rev Pathol* (2019) 14:421–47. doi: 10.1146/annurev-pathol-020117-043711
- Stein C, Migliavaca CB, Colpani V, da Rosa PR, Sganzerla D, Giordani NE, et al. Amiodarone for arrhythmia in patients with Chagas disease: A systematic review and individual patient data meta-analysis. *PLoS Negl Trop Dis* (2018) 12:e0006742. doi: 10.1371/journal.pntd.0006742
- Benaïm G, Paniz Mondolfi AE. The emerging role of amiodarone and dronedarone in Chagas disease. *Nat Rev Cardiol* (2012) 9:605–9. doi: 10.1038/nrcardio.2012.108
- Mujović N, Dobrev D, Marinković M, Russo V, Potpara TS. The role of amiodarone in contemporary management of complex cardiac arrhythmias. *Pharmacol Res* (2020) 151:104521. doi: 10.1016/j.phrs.2019.104521
- Hamilton D Sr, Nandkeolyar S, Lan H, Desai P, Evans J, Hauschild C, et al. Amiodarone: A comprehensive guide for clinicians. *Am J Cardiovasc Drugs* (2020) 20:549–58. doi: 10.1007/s40256-020-00401-5
- Elnaggar MN, Jbeili K, Nik-Hussain N, Kozhippally M, Pappachan JM. Amiodarone-induced thyroid dysfunction: A clinical update. *Exp Clin Endocrinol Diabetes* (2018) 126:333–41. doi: 10.1055/a-0577-7574
- Colunga Biancatelli RM, Congedo V, Calvosa L, Ciacciarelli M, Polidoro A, Iuliano L. Adverse reactions of amiodarone. *J Geriatr Cardiol* (2019) 16:552–66. doi: 10.11909/j.issn.1671-5411.2019.07.004
- Feduska ET, Thoma BN, Torjman MC, Goldhammer JE. Acute amiodarone pulmonary toxicity. *J Cardiothorac Vasc Anesth* (2021) 35:1485–94. doi: 10.1053/j.jvca.2020.10.060
- Hubel E, Fishman S, Holopainen M, Käkälä R, Shaffer O, Houry I, et al. Repetitive amiodarone administration causes liver damage via adipose tissue ER stress-dependent lipolysis, leading to hepatotoxic free fatty acid accumulation. *Am J Physiol Gastrointest Liver Physiol* (2021) 321:G298–307. doi: 10.1152/ajpgi.00458.2020
- European Medicines Agency. *MULTAQ product-information -Annex I Summary of Product Characteristics* (2011). Available at: [https://www.ema.europa.eu/en/documents/other/multiq-product-information-approved-chmp-22-september-2011-pending-endorsement-european-commission\\_en.pdf](https://www.ema.europa.eu/en/documents/other/multiq-product-information-approved-chmp-22-september-2011-pending-endorsement-european-commission_en.pdf) (Accessed June 20, 2023).
- Vaughan Williams EM. Classification of antidysrhythmic drugs. *Pharmacology & Therapeutics. Part B: Gen Systematic Pharmacol* (1975) 1(1):115–38. doi: 10.1016/0306-039x(75)90019-7

## Acknowledgments

We wish to thank Epichem Pty Ltd for their help in the provision of the chemicals and compounds necessary for this study and for the synthesis of benzimidazole used in both *in vitro* and *in vivo* studies described in this manuscript. We also wish to thank DNDi partners that have been involved in the *in vitro* screening of compounds during the years, in particular LMPH laboratory at University of Antwerp, Belgium, STPH in Basel, Switzerland, Institute Pasteur Korea, South Korea, and Dundee Discovery Unit, Dundee, UK.

## Conflict of interest

The authors declare that the research was conducted in the absence of any commercial or financial relationships that could be construed as a potential conflict of interest.

## Publisher's note

All claims expressed in this article are solely those of the authors and do not necessarily represent those of their affiliated organizations, or those of the publisher, the editors and the reviewers. Any product that may be evaluated in this article, or claim that may be made by its manufacturer, is not guaranteed or endorsed by the publisher.

## Supplementary material

The Supplementary Material for this article can be found online at: <https://www.frontiersin.org/articles/10.3389/fitd.2023.1254061/full#supplementary-material>

17. Wilkinson SR, Bot C, Kelly JM, Hall BS. Trypanocidal activity of nitroaromatic prodrugs: current treatments and future perspectives. *Curr Top Med Chem* (2011) 11:2072–84. doi: 10.2174/156802611796575894
18. Torrico F, Gascón J, Barreira F, Blum B, Almeida IC, Alonso-Vega C, et al. BENDITA study group. New regimens of benznidazole monotherapy and in combination with fosravuconazole for treatment of Chagas disease (BENDITA): a phase 2, double-blind, randomised trial. *Lancet Infect Dis* (2021) 21:1129–40. doi: 10.1016/S1473-3099(20)30844-6
19. Sales Junior PA, Molina I, Fonseca Murta SM, Sánchez-Montalvá A, Salvador F, Corrêa-Oliveira R, et al. Experimental and clinical treatment of Chagas disease: A review. *Am J Trop Med Hyg* (2017) 97:1289–303. doi: 10.4269/ajtmh.16-0761
20. Molina-Berrios A, Campos-Estrada C, Lapier M, Duaso J, Kemmerling U, Galanti N, et al. Benznidazole prevents endothelial damage in an experimental model of Chagas disease. *Acta Trop* (2013) 27:6–13. doi: 10.1016/j.actatropica.2013.03.006
21. Calvet CM, Choi JY, Thomas D, Suzuki B, Hirata K, Lostracco-Johnson S, et al. 4-aminopyridyl-based lead compounds targeting CYP51 prevent spontaneous parasite relapse in a chronic model and improve cardiac pathology in an acute model of *Trypanosoma cruzi* infection. *PLoS Negl Trop Dis* (2017) 11:e0006132. doi: 10.1371/journal.pntd.0006132
22. Francisco AF, Jayawardhana S, Taylor MC, Lewis MD, Kelly JM. Assessing the effectiveness of curative benznidazole treatment in preventing chronic cardiac pathology in experimental models of Chagas disease. *Antimicrob Agents Chemother* (2018) 62:e00832–18. doi: 10.1128/AAC.00832-18
23. Peña I, Pilar Manzano M, Cantizani J, Kessler A, Alonso-Padilla J, Bardera AI, et al. New compound sets identified from high throughput phenotypic screening against three kinetoplastid parasites: an open resource. *Sci Rep* (2015) 5:8771. doi: 10.1038/srep08771
24. Chatelain E, Ioset JR. Phenotypic screening approaches for Chagas disease drug discovery. *Expert Opin Drug Discovery* (2018) 13:141–53. doi: 10.1080/17460441.2018.1417380
25. Benaim G, Sanders JM, Garcia-Marchán Y, Colina C, Lira R, Caldera AR, et al. Amiodarone has intrinsic anti-*Trypanosoma cruzi* activity and acts synergistically with posaconazole. *J Med Chem* (2006) 49:892–9. doi: 10.1021/jm050691f
26. Adesse D, Azzam EM, Meirelles Mde N, Urbijá JA, Garzoni LR. Amiodarone inhibits *Trypanosoma cruzi* infection and promotes cardiac cell recovery with gap junction and cytoskeleton reassembly in vitro. *Antimicrob Agents Chemother* (2011) 55:203–10. doi: 10.1128/AAC.01129-10
27. Benaim G, Hernandez-Rodriguez V, Mujica-Gonzalez S, Plaza-Rojas L, Silva ML, Parra-Gimenez N, et al. In vitro anti-*Trypanosoma cruzi* activity of dronedarone, a novel amiodarone derivative with an improved safety profile. *Antimicrob Agents Chemother* (2012) 56:3720–5. doi: 10.1128/AAC.00207-12
28. Veiga-Santos P, Barrias ES, Santos JF, de Barros Moreira TL, de Carvalho TM, Urbina JA, et al. Effects of amiodarone and posaconazole on the growth and ultrastructure of *Trypanosoma cruzi*. *Int J Antimicrob Agents* (2012) 40:61–71. doi: 10.1016/j.ijantimicag.2012.03.009
29. Lourenço AM, Faccini CC, Costa CAJ, Mendes GB, Fragata Filho AA. Evaluation of in vitro anti-*Trypanosoma cruzi* activity of medications benznidazole, amiodarone hydrochloride, and their combination. *Rev Soc Bras Med Trop* (2018) 51:52–6. doi: 10.1590/0037-8682-0285-2017
30. Sass G, Madigan RT, Joubert LM, Bozzi A, Sayed N, Wu JC, et al. A combination of itraconazole and amiodarone is highly effective against *Trypanosoma cruzi* infection of human stem cell-derived cardiomyocytes. *Am J Trop Med Hyg* (2019) 101:383–91. doi: 10.4269/ajtmh.19-0023
31. Benaim G, Paniz-Mondolfi AE, Sordillo EM, Martinez-Sotillo N. Disruption of intracellular calcium homeostasis as a therapeutic target against *Trypanosoma cruzi*. *Front Cell Infect Microbiol* (2020) 10:46. doi: 10.3389/fcimb.2020.00046
32. Benaim G, Paniz-Mondolfi AE, Sordillo EM. The rationale for use of amiodarone and its derivatives for the treatment of chagas' Disease and leishmaniasis. *Curr Pharm Des* (2021) 27(15):1825–33. doi: 10.2174/1381612826666200928161403
33. Carmo AA, Rocha MO, Silva JL, Ianni BM, Fernandes F, Sabino EC, et al. Amiodarone and *Trypanosoma cruzi* parasitemia in patients with Chagas disease. *Int J Cardiol* (2015) 189:182–4. doi: 10.1016/j.ijcard.2015.04.061
34. Francisco AF, Jayawardhana S, Lewis MD, White KL, Shackelford DM, Chen G, et al. Nitroheterocyclic drugs cure experimental *Trypanosoma cruzi* infections more effectively in the chronic stage than in the acute stage. *Sci Rep* (2016) 6:35351. doi: 10.1038/srep35351
35. Riccardi K, Cawley S, Yates PD, Chang C, Funk C, Niosi M, et al. Plasma protein binding of challenging compounds. *J Pharm Sci* (2015) 104:2627–36. doi: 10.1002/jps.24506
36. Gabaldón-Figueira JC, Martínez-Peinado N, Escabia E, Ros-Lucas A, Chatelain E, Scandale I, et al. State-of-the-art in the drug discovery pathway for chagas disease: A framework for drug development and target validation. *Res Rep Trop Med* (2023) 14:1–19. doi: 10.2147/RRTM.S415273
37. Lewis MD, Fortes Francisco A, Taylor MC, Kelly JM. A new experimental model for assessing drug efficacy against *Trypanosoma cruzi* infection based on highly sensitive in vivo imaging. *J Biomolecular Screening* (2015) 20:36–43. doi: 10.1177/1087057114552623
38. Barbosa JMC, Pedra-Rezende Y, de Melo TG, de Oliveira G, Cascabulho CM, Pereira ENGDS, et al. Experimental combination therapy with amiodarone and low-dose benznidazole in a mouse model of *Trypanosoma cruzi* acute infection. *Microbiol Spectr* (2022) 10(1):e0185221. doi: 10.1128/spectrum.01852-21
39. Madigan R, Majoy S, Ritter K, Concepción JL, Márquez ME, Caribay Silva S, et al. Investigation of a combination of amiodarone and itraconazole for treatment of American trypanosomiasis (Chagas disease) in dogs. *J Am Vet Med Assoc* (2019) 255(3):317–29. doi: 10.2460/javma.255.3.317
40. Food and Drug Administration database. *Cordarone® (amiodarone HCl) tablets product label* (2010). Available at: [https://www.accessdata.fda.gov/drugsatfda\\_docs/label/2010/018972s042lbl](https://www.accessdata.fda.gov/drugsatfda_docs/label/2010/018972s042lbl) (Accessed June 20, 2023). Reference ID: 2876651.
41. Freedman MD, Somberg JC. Pharmacology and pharmacokinetics of amiodarone. *J Clin Pharmacol* (1991) 31(11):1061–9. doi: 10.1002/j.1552-4604.1991.tb03673.x
42. Latini R, Tognoni G, Kates RE. Clinical pharmacokinetics of amiodarone. *Clin Pharmacokinet* (1984) 9(2):136–56. doi: 10.2165/00003088-198409020-00002
43. Haffajee CI, Love JC, Canada AT, Lesko LJ, Asdourian G, Alpert JS. Clinical pharmacokinetics and efficacy of amiodarone for refractory tachyarrhythmias. *Circulation* (1983) 67(6):1347–55. doi: 10.1161/01.cir.67.6.1347
44. Food and Drug Administration database. *MULTAQ (dronedarone) prescribing information* (2009). Available at: [https://www.accessdata.fda.gov/drugsatfda\\_docs/label/2009/022425lbl.pdf](https://www.accessdata.fda.gov/drugsatfda_docs/label/2009/022425lbl.pdf) (Accessed June 20, 2023).
45. Bostanitis I, Tsalidou M. Pharmacokinetics of dronedarone, in: *Front. Pharmacol. Conference Abstract: 8th Southeast European Congress on Xenobiotic Metabolism and Toxicity - XEMET*. (2010). doi: 10.3389/conf.fphar.2010.60.00108
46. Sykes ML, Avery VM. Development and application of a sensitive, phenotypic, high-throughput image-based assay to identify compound activity against *Trypanosoma cruzi* amastigotes. *Int J Parasitol Drugs Drug Resist* (2015) 5(3):215–28. doi: 10.1016/j.ijpddr.2015.10.001
47. De Rycker M, Thomas J, Riley J, Brough SJ, Miles TJ, Gray DW. Identification of Trypanocidal activity for known clinical compounds using a new *Trypanosoma cruzi* hit-discovery screening cascade. *PLoS Negl Trop Dis* (2016) 10(4):e0004584. doi: 10.1371/journal.pntd.0004584
48. Koovits PJ, Dessoy MA, Matheeußen A, Maes L, Caljon G, Mowbray CE, et al. Structure-activity relationship of 4-azaindole-2-piperidine derivatives as agents against *Trypanosoma cruzi*. *Bioorg Med Chem Lett* (2020) 30(1):126779. doi: 10.1016/j.bmcl.2019.126779
49. Yang G, Lee N, Ioset JR, No JH. Evaluation of parameters impacting drug susceptibility in intracellular *Trypanosoma cruzi* assay protocols. *SLAS Discovery* (2017) 22(2):125–34. doi: 10.1177/1087057116673796
50. Costa FC, Francisco AF, Jayawardhana S, Calderano SG, Lewis MD, Olmo F, et al. Expanding the toolbox for *Trypanosoma cruzi*: A parasite line incorporating a bioluminescence-fluorescence dual reporter and streamlined CRISPR/Cas9 functionality for rapid in vivo localisation and phenotyping. *PLoS Negl Trop Dis* (2018) 12:e0006388. doi: 10.1371/journal.pntd.0006388
51. Scarim CB, Olmo F, Ferreira EI, Chin CM, Kelly JM, Francisco AF. Image-based in vitro screening reveals the trypanostatic activity of hydroxymethylnitrofurazone against *trypanosoma cruzi*. *Int J Mol Sci* (2021) 22(13):6930. doi: 10.3390/ijms22136930
52. Branchini BR, Ablamsky DM, Davis AL, Southworth TL, Butler B, Fan F, et al. Red-emitting luciferases for bioluminescence reporter and imaging applications. *Anal Biochem* (2010) 396:290–7. doi: 10.1016/j.ab.2009.09.009
53. Lewis MD, Francisco AF, Taylor MC, Burrell-Saward H, McLatchie AP, Miles MA, et al. Bioluminescence imaging of chronic *Trypanosoma cruzi* infections reveals tissue-specific parasite dynamics and heart disease in the absence of locally persistent infection. *Cell Microbiol* (2014) 16(9):1285–300. doi: 10.1111/cmi.12297
54. Kalvass C, Maurer TS. Influence of nonspecific brain and plasma binding on CNS exposure: implications for rational drug discovery. *Biopharm Drug Dispos* (2002) 23:327–38. doi: 10.1002/bdd.325